

PDF hosted at the Radboud Repository of the Radboud University Nijmegen

The following full text is a publisher's version.

For additional information about this publication click this link.

<http://hdl.handle.net/2066/124592>

Please be advised that this information was generated on 2021-10-18 and may be subject to change.



ELSEVIER

22 February 1996

PHYSICS LETTERS B

Physics Letters B 369 (1996) 163–172

Measurement of the $\tau^- \rightarrow e^- \bar{\nu}_e \nu_\tau$ branching ratio

OPAL Collaboration

G. Alexander^w, J. Allison^p, N. Altekamp^e, K. Ametewee^y, K.J. Andersonⁱ, S. Anderson^l, S. Arcelli^b, S. Asai^x, D. Axen^{ac}, G. Azuelos^{r,1}, A.H. Ball^q, E. Barberio^z, R.J. Barlow^p, R. Bartoldus^c, J.R. Batley^e, G. Beaudoin^r, J. Bechtluftⁿ, G.A. Beck^m, C. Beeston^p, T. Behnke^h, A.N. Bell^a, K.W. Bell^t, G. Bella^w, S. Bentvelsen^h, P. Berlich^j, S. Bethkeⁿ, O. Biebelⁿ, I.J. Bloodworth^a, J.E. Bloomer^a, P. Bock^k, H.M. Bosch^k, M. Boutemour^r, B.T. Bouwens^l, S. Braibant^l, P. Bright-Thomas^y, R.M. Brown^t, H.J. Burckhart^h, C. Burgard^{aa}, R. Bürgin^j, P. Capiluppi^b, R.K. Carnegie^f, A.A. Carter^m, J.R. Carter^e, C.Y. Chang^q, C. Charlesworth^f, D.G. Charlton^{a,2}, D. Chrisman^d, S.L. Chu^d, P.E.L. Clarke^o, S.G. Clowes^p, I. Cohen^w, J.E. Conboy^o, O.C. Cooke^p, M. Cuffiani^b, S. Dado^v, C. Dallapiccola^q, G.M. Dallavalle^b, C. Darling^{ae}, S. De Jong^l, L.A. del Pozo^h, M.S. Dixit^g, E. do Couto e Silva^l, E. Duchovni^z, G. Duckeck^h, I.P. Duerdoth^p, U.C. Dunwoody^h, J.E.G. Edwards^p, P.G. Estabrooks^f, H.G. Evansⁱ, F. Fabbri^b, B. Fabbro^u, P. Fath^k, F. Fiedler^l, M. Fierro^b, M. Fincke-Keeler^{ab}, H.M. Fischer^c, R. Folman^z, D.G. Fong^q, M. Foucher^q, H. Fukui^x, A. Fürties^h, P. Gagnon^g, A. Gaidot^u, J.W. Gary^d, J. Gascon^r, S.M. Gascon-Shotkin^q, N.I. Geddes^t, C. Geich-Gimbel^c, S.W. Genslerⁱ, F.X. Gentit^u, T. Geralis^t, G. Giacomelli^b, P. Giacomelli^d, R. Giacomelli^b, V. Gibson^e, W.R. Gibson^m, D.M. Gingrich^{ad,1}, J. Goldberg^v, M.J. Goodrick^e, W. Gorn^d, C. Grandi^b, E. Gross^z, C. Hajdu^{af}, G.G. Hanson^l, M. Hansroul^h, M. Hapke^m, C.K. Hargrove^g, P.A. Hartⁱ, C. Hartmann^c, M. Hauschild^h, C.M. Hawkes^h, R. Hawkings^h, R.J. Hemingway^f, G. Herten^j, R.D. Heuer^h, M.D. Hildreth^h, J.C. Hill^e, S.J. Hillier^h, T. Hilse^j, P.R. Hobson^y, D. Hochman^z, R.J. Homer^a, A.K. Honma^{ab,1}, D. Horváth^{af,3}, R. Howard^{ac}, R.E. Hughes-Jones^p, D.E. Hutchcroft^e, P. Igo-Kemenes^k, D.C. Imrie^y, A. Jawahery^q, P.W. Jeffreys^t, H. Jeremie^r, M. Jimack^a, A. Joly^r, M. Jones^f, R.W.L. Jones^h, U. Jost^k, P. Jovanovic^a, D. Karlen^f, T. Kawamoto^x, R.K. Keeler^{ab}, R.G. Kellogg^q, B.W. Kennedy^t, B.J. King^h, J. King^m, J. Kirk^{ac}, S. Kluth^e, T. Kobayashi^x, M. Kobel^j, D.S. Koetke^f, T.P. Kokott^c, S. Komamiya^x, R. Kowalewski^h, T. Kress^k, P. Krieger^f, J. von Krogh^k, P. Kyberd^m, G.D. Lafferty^p, H. Lafoux^u, R. Lahmann^q, W.P. Lai^s, D. Lanskeⁿ, J. Lauber^o, J.G. Layter^d, A.M. Lee^{ae}, E. Lefebvre^r, D. Lellouch^z, J. Letts^b, L. Levinson^z, C. Lewis^o, S.L. Lloyd^m, F.K. Loebinger^p, G.D. Long^q, B. Lorazo^r, M.J. Losty^g, J. Ludwig^j, A. Luig^j, A. Malik^u, M. Mannelli^h, S. Marcellini^b

C. Markus^c, A.J. Martin^m, J.P. Martin^r, G. Martinez^q, T. Mashimo^x, W. Matthews^y,
 P. Mättig^c, W.J. McDonald^{ad}, J. McKenna^{ac}, E.A. Mckigney^o, T.J. McMahon^a,
 A.I. McNab^m, F. Meijers^h, S. Menke^c, F.S. Merrittⁱ, H. Mes^g, J. Meyer^{aa}, A. Michelini^h,
 G. Mikenberg^z, D.J. Miller^o, R. Mir^z, W. Mohr^j, A. Montanari^b, T. Mori^x, M. Morii^x,
 U. Müller^c, B. Nellen^c, B. Nijjhar^p, R. Nisius^h, S.W. O’Neale^a, F.G. Oakham^g,
 F. Odorici^b, H.O. Ogren^l, N.J. Oldershaw^p, T. Omori^x, C.J. Oram^{ab,1}, M.J. Oregliaⁱ,
 S. Orito^x, M. Palazzo^b, J. Pálincás^{ag}, J.P. Pansart^u, G. Pásztor^{ag}, J.R. Pater^p,
 G.N. Patrick^t, M.J. Pearce^a, P.D. Phillips^p, J.E. Pilcherⁱ, J. Pinfold^{ad}, D.E. Plane^h,
 P. Poffenberger^{ab}, B. Poli^b, A. Posthaus^c, T.W. Pritchard^m, H. Przysiezniak^{ad}, D.L. Rees^a,
 D. Rigby^a, M.G. Rison^e, S.A. Robins^m, N. Rodning^{ad}, J.M. Roney^{ab}, E. Ros^h,
 A.M. Rossi^b, M. Rosvick^{ab}, P. Routenburg^{ad}, Y. Rozen^h, K. Runge^j, O. Runolfsson^h,
 D.R. Rust^l, R. Rylko^y, E.K.G. Sarkisyan^w, M. Sasaki^x, C. Sbarra^b, A.D. Schaile^h,
 O. Schaile^j, F. Scharf^c, P. Scharff-Hansen^h, P. Schenk^d, B. Schmitt^c, M. Schröder^h,
 H.C. Schultz-Coulon^j, M. Schulz^h, P. Schütz^c, J. Schwiening^c, W.G. Scott^t, T.G. Shears^p,
 B.C. Shen^d, C.H. Shepherd-Themistocleous^{aa}, P. Sherwood^o, G.P. Siroli^b, A. Sittler^{aa},
 A. Skillman^o, A. Skuja^q, A.M. Smith^h, T.J. Smith^{ab}, G.A. Snow^q, R. Sobie^{ab},
 S. Söldner-Rembold^j, R.W. Springer^{ad}, M. Sproston^t, A. Stahl^c, M. Starks^l, C. Stegmann^j,
 K. Stephens^p, J. Steuerer^{ab}, B. Stockhausen^c, D. Strom^s, F. Strumia^h, P. Szymanski^t,
 R. Tafirout^r, H. Takeda^x, P. Taras^r, S. Tarem^z, M. Tecchio^h, N. Tesch^c, M.A. Thomson^h,
 E. von Törne^c, S. Towers^f, M. Tscheulin^j, T. Tsukamoto^x, E. Tsur^w, A.S. Turcotⁱ,
 M.F. Turner-Watson^h, P. Utzat^k, R. Van Kooten^l, G. Vasseur^u, P. Vikas^r, M. Vinciter^{ab},
 E.H. Vokurka^p, F. Wäckerle^j, A. Wagner^{aa}, D.L. Wagnerⁱ, C.P. Ward^e, D.R. Ward^e,
 J.J. Ward^o, P.M. Watkins^a, A.T. Watson^a, N.K. Watson^g, P. Weber^f, P.S. Wells^h,
 N. Vermes^c, B. Wilkens^j, G.W. Wilson^{aa}, J.A. Wilson^a, T. Wlodek^z, G. Wolf^z,
 S. Wotton^k, T.R. Wyatt^p, S. Xella^b, S. Yamashita^x, G. Yekutieli^z, V. Zacek^r

^a School of Physics and Space Research, University of Birmingham, Birmingham B15 2TT, UK

^b Dipartimento di Fisica dell’ Università di Bologna and INFN, I-40126 Bologna, Italy

^c Physikalisches Institut, Universität Bonn, D-53115 Bonn, Germany

^d Department of Physics, University of California, Riverside CA 92521, USA

^e Cavendish Laboratory, Cambridge CB3 0HE, UK

^f Ottawa-Carleton Institute for Physics, Department of Physics, Carleton University, Ottawa, Ontario K1S 5B6, Canada

^g Centre for Research in Particle Physics, Carleton University, Ottawa, Ontario K1S 5B6, Canada

^h CERN, European Organisation for Particle Physics, CH-1211 Geneva 23, Switzerland

ⁱ Enrico Fermi Institute and Department of Physics, University of Chicago, Chicago IL 60637, USA

^j Fakultät für Physik, Albert Ludwigs Universität, D-79104 Freiburg, Germany

^k Physikalisches Institut, Universität Heidelberg, D-69120 Heidelberg, Germany

^l Indiana University, Department of Physics, Swain Hall West 117, Bloomington IN 47405, USA

^m Queen Mary and Westfield College, University of London, London E1 4NS, UK

ⁿ Technische Hochschule Aachen, III Physikalisches Institut, Sommerfeldstrasse 26-28, D-52056 Aachen, Germany

^o University College London, London WC1E 6BT, UK

^p Department of Physics, Schuster Laboratory, The University, Manchester M13 9PL, UK

^q Department of Physics, University of Maryland, College Park, MD 20742, USA

^r Laboratoire de Physique Nucléaire, Université de Montréal, Montréal, Quebec H3C 3J7, Canada

^s University of Oregon, Department of Physics, Eugene OR 97403, USA

^t Rutherford Appleton Laboratory, Chilton, Didcot, Oxfordshire OX11 0QX, UK

^u CEA, DAPNIA/SPP, CE-Saclay, F-91191 Gif-sur-Yvette, France

^v Department of Physics, Technion-Israel Institute of Technology, Haifa 32000, Israel

^w Department of Physics and Astronomy, Tel Aviv University, Tel Aviv 69978, Israel

^x International Centre for Elementary Particle Physics and Department of Physics, University of Tokyo, Tokyo 113, Japan
and Kobe University, Kobe 657, Japan

^y Brunel University, Uxbridge, Middlesex UB8 3PH, UK

^z Particle Physics Department, Weizmann Institute of Science, Rehovot 76100, Israel

^{aa} Universität Hamburg/DESY, II Institut für Experimental Physik, Notkestrasse 85, D-22607 Hamburg, Germany

^{ab} University of Victoria, Department of Physics, P O Box 3055, Victoria BC V8W 3P6, Canada

^{ac} University of British Columbia, Department of Physics, Vancouver BC V6T 1Z1, Canada

^{ad} University of Alberta, Department of Physics, Edmonton AB T6G 2J1, Canada

^{ae} Duke University, Department of Physics, Durham, NC 27708-0305, USA

^{af} Research Institute for Particle and Nuclear Physics, H-1525 Budapest, P O Box 49, Hungary

^{ag} Institute of Nuclear Research, H-4001 Debrecen, P O Box 51, Hungary

Received 4 October 1995

Editor: K. Winter

Abstract

The branching ratio of the $\tau^- \rightarrow e^- \bar{\nu}_e \nu_\tau$ decay mode has been measured with the OPAL detector to be $(17.78 \pm 0.10 \pm 0.09)\%$ where the first error is statistical and the second is systematic. The branching ratio, together with other measurements, has been used to test $e - \mu$ and $\mu - \tau$ universality in the charged current weak interaction.

1. Introduction

The $\tau^- \rightarrow e^- \bar{\nu}_e \nu_\tau$ decay is a useful probe of the Standard Model. The branching ratio, in conjunction with other measurements, can be used to determine the relative charged current couplings of the electron, muon and tau leptons. In addition, it can be used to calculate α_s at $Q^2 = M_\tau^2$, which can be compared with other measurements taken at $Q^2 = M_Z^2$. This letter reports on an update of the $\tau^- \rightarrow e^- \bar{\nu}_e \nu_\tau$ branching ratio using the data collected between 1991 and 1994 with the OPAL detector at LEP.

The data were recorded using the OPAL detector which is a general purpose detector covering the full solid angle [1]. The tau pair Monte Carlo sample was generated using the KORALZ 4.0 package [2]. The dynamics of the tau decays were simulated with the TAUOLA 2.0 decay library [3]. The Monte Carlo events were then passed through the GEANT simulation [4] of the OPAL detector [5].

2. Selection of $\tau^+\tau^-$ events

The procedure used to select $Z^0 \rightarrow \tau^+\tau^-$ events is similar to that described in previous OPAL publications [6–8]. The decay of the Z^0 produces two back-to-back taus. The taus are highly relativistic so that the decay products are strongly collimated. As a result it is convenient to treat each τ decay as a jet, as defined in Ref. [9], where charged tracks and clusters in the lead-glass electromagnetic calorimeter are assigned to cones of half-angle 35° . The definitions of a charged track and electromagnetic cluster are also given in Refs. [6–8]. The tau pair selection requires that the event contains exactly two jets each with at least one charged track. The total electromagnetic energy plus the sum of the scalar momentum of the charged tracks in each jet must exceed 1% of the beam energy. The average value of $|\cos\theta|$ for the two charged jets must satisfy $|\cos\theta| < 0.68$, where θ is the polar angle.

The background in the $\tau^+\tau^-$ sample includes contributions from the $e^+e^- \rightarrow e^+e^-$ [10], $e^+e^- \rightarrow \mu^+\mu^-$ [2], $e^+e^- \rightarrow q\bar{q}$ [11] and $e^+e^- \rightarrow (e^+e^-)X$ [12] reactions. The background from $e^+e^- \rightarrow e^+e^-$ events is reduced by requiring the tau pair candidates to satisfy either $E_{\text{cluster}} \leq 0.8E_{\text{CM}}$ or $E_{\text{cluster}} + 0.3E_{\text{track}} \leq$

¹ Also at TRIUMF, Vancouver, Canada V6T 2A3.

² Royal Society University Research Fellow.

³ Institute of Nuclear Research, Debrecen, Hungary.

E_{CM} , where E_{cluster} is the total energy in the lead-glass calorimeter and E_{track} is the sum of the scalar momentum of the charged tracks in the event. Events from the $e^+e^- \rightarrow \mu^+\mu^-$ reaction, multihadronic decays of the Z^0 ($e^+e^- \rightarrow q\bar{q}$) and $e^+e^- \rightarrow (e^+e^-)X$ (two-photon) events are rejected using requirements identical to those described in Ref. [8].

The fraction of background in the tau pair sample is found to be 0.0170 ± 0.0012 . The contributions from the individual channels are given in Table 1. The $e^+e^- \rightarrow q\bar{q}$ and $e^+e^- \rightarrow (e^+e^-)\mu^+\mu^-$ background estimates have not changed from Ref. [8]. The $e^+e^- \rightarrow \mu^+\mu^-$, $e^+e^- \rightarrow e^+e^-$ and $e^+e^- \rightarrow (e^+e^-)e^+e^-$ backgrounds have been re-evaluated since they are a significant background in either the tau pair sample or the $\tau^- \rightarrow e^-\bar{\nu}_e\nu_\tau$ sample. The backgrounds have been estimated by Monte Carlo and confirmed by comparisons with data in a manner similar to that presented in Ref. [8]. These selection criteria were applied to all the data collected from 1991 to 1994 to give a sample of 82808 $\tau^+\tau^-$ candidate events.

3. Selection of electron candidates

The selection of electron candidates is divided into two parts: a ‘fiducial’ selection followed by an ‘electron identification’ selection. The fiducial selection applies criteria that are independent of the particle type (such as fiducial cuts). The efficiency for this selection is determined entirely from data samples. The electron identification selection applies criteria that separate electrons from muons and hadrons. For this selection the efficiency is estimated using Monte Carlo samples and systematic studies comparing data and Monte Carlo samples are done to estimate the uncertainty.

The fiducial selection requires that the candidate jet have between 1 and 3 charged tracks. Regions of the detector where the z -measuring tracking chamber or ‘ z -chamber’⁴ was not active and the regions of poor energy resolution in the electromagnetic calorimeter

⁴ A right-handed coordinate system is adopted in OPAL, where the x axis points to the centre of the LEP ring, and positive z is along the electron beam direction. The angles θ and ϕ are the polar and azimuthal angles, respectively.

Table 1
Estimated backgrounds after applying corrections

Background	Corrected contamination τ pairs
$e^+e^- \rightarrow \mu^+\mu^-$	0.0072 ± 0.0005
$e^+e^- \rightarrow q\bar{q}$	0.0042 ± 0.0008
$e^+e^- \rightarrow e^+e^-$	0.0041 ± 0.0007
$e^+e^- \rightarrow (e^+e^-)\mu^+\mu^-$	0.0008 ± 0.0002
$e^+e^- \rightarrow (e^+e^-)e^+e^-$	0.0007 ± 0.0002
Total	0.0170 ± 0.0012
Background	Corrected contamination $\tau^- \rightarrow e^-\bar{\nu}_e\nu_\tau$
$\tau^- \rightarrow h^- \geq 1\pi^0\nu_\tau$	0.0253 ± 0.0020
$\tau^- \rightarrow h^-\nu_\tau$	0.0139 ± 0.0017
$e^+e^- \rightarrow e^+e^-$	0.0057 ± 0.0013
$e^+e^- \rightarrow (e^+e^-)e^+e^-$	0.0038 ± 0.0011
other τ decays	0.0009 ± 0.0004
Total	0.0496 ± 0.0031

are eliminated. Also, we apply additional requirements to the tracks. The highest momentum track in each jet, assumed to be the electron candidate, must have hits in the z -chambers in order to improve the polar angular resolution. In addition, we require that each track have at least 40 hits in the central drift chamber that can be used in the measurement of the energy loss (dE/dx).

The efficiencies for the fiducial selection were determined using the entire tau data sample and are given in Table 2. Note that the efficiencies for the z -chamber and dE/dx -hits used in the branching ratio calculation were determined as a function of momentum but only average values are given in Table 2. The z -chamber and dE/dx hit efficiencies for jets with 1 charged track were tested to see if they were independent of the particle type using control samples of electron data. The systematic errors quoted on these efficiencies (see Table 2) represents the precision with which this assumption was tested.

The electron identification selection identifies the electron candidates out of the tau sample remaining after the fiducial selection. The electron identification selection relies on a relatively small set of variables in order to achieve high efficiency with low background. A number of the variables have been transformed into normalized quantities, $N_V^g \equiv (V_{\text{measured}} - V_{\text{expected}}) / \sigma_V$, where V_{measured} is the variable of interest, V_{expected} is

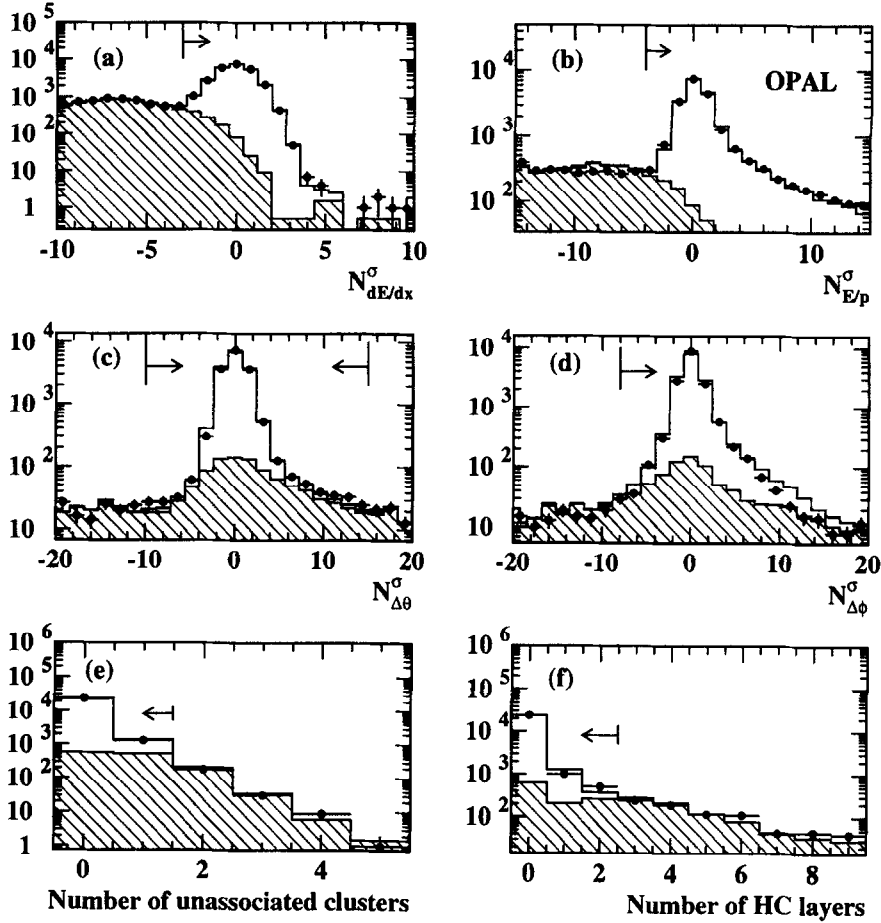


Fig. 1. The main variables used in the electron selection are plotted: (a) the normalized dE/dx , (b) the normalized E/p , (c) the normalized $\Delta\theta$, (d) the normalized $\Delta\phi$, (e) the number of clusters not associated to a charged track and (f) the number of hadron calorimeter layers. The data are represented by points and the Monte Carlo prediction is represented by the unshaded histogram. The shaded region of the histogram is the Monte Carlo prediction for the background. The data shown in each plot are required to pass the electron selection except for the variable displayed. The arrows indicate the regions accepted in the selection.

Table 2
Efficiencies of fiducial selection

Description	Efficiency
z -chamber acceptance	0.93905 ± 0.00066
EM calorimeter acceptance	0.9835 ± 0.0004
z -chamber hits (1 tk) ^a	$0.91619 \pm 0.00079 \pm 0.00160$
z -chamber hits (2, 3 tk)	0.85 ± 0.05
dE/dx hits (1 tk) ^a	$0.99210 \pm 0.00024 \pm 0.00050$
dE/dx hits (2 tk)	1.00 ± 0.05
dE/dx hits (3 tk)	0.90 ± 0.05

^a Here we give the average efficiency whereas in the actual selection the momentum dependent efficiency is used.

the expected mean value and σ_V is its rms.

The electron candidates are required to pass the following criteria:

- The charged track must have a dE/dx measurement ($N_{dE/dx}^\sigma \geq -3$) compatible with that expected from an electron (see Fig. 1(a)).
- The energy of the cluster (E) associated to the track divided by the momentum of the track (p) must be close to unity (equivalently $N_{E/p}^\sigma \geq -4$ as shown in Fig. 1(b)).
- The difference in the position of the track and associated cluster is required to be less than a few milliradians. This is achieved by placing re-

quirements on the $N_{\Delta\theta}^{\sigma}$ and $N_{\Delta\phi}^{\sigma}$ distributions (see Figs. 1(c) and (d)), where $\Delta\theta = \theta_{rk} - \theta_{cl}$ and $\Delta\phi = \phi_{rk} - \phi_{cl}$. The matching in ϕ is complicated by the magnetic field and by photon radiation, so a looser matching criterion is applied in ϕ than in θ .

- (d) We require that there are less than two photons in the jet (see Fig. 1(e)). A cluster is considered a photon candidate if its energy is greater than 0.7 GeV and it is not associated to a charged track.
- (e) We require that the electron candidate penetrate no further than 2 layers (0.6 interaction lengths) into the hadron calorimeter (see Fig. 1(f)).
- (f) Residual $e^+e^- \rightarrow e^+e^-$ background is reduced by requiring that $\theta_{\text{acop}} > 0.002$ radians if both $p > 30$ GeV/c and $p_{\text{opp}} > 0.75E_{\text{beam}}$, where θ_{acop} is the acoplanarity angle in the plane transverse to the beam between the highest momentum tracks in each jet, p is the momentum of the electron candidate, p_{opp} is the momentum of the track in the jet opposite the electron candidate and E_{beam} is the beam energy.
- (g) If the jet contains 2 or 3 charged tracks, then we assume that highest momentum track is the electron. In order for the event to be considered an electron candidate, simple cuts are applied to the remaining track(s) to ensure that they are consistent with coming from a photon conversion.

4. Branching ratio determination

A total of 25 337 candidates pass the electron selection with an electron identification efficiency, ϵ_E , of 0.9893 ± 0.0027 and a background, $f_{\text{bkgd}}^{\text{non-e}}$, of 0.0496 ± 0.0031 . These results give a branching ratio of the $\tau^- \rightarrow e^- \bar{\nu}_e \nu_{\tau}$ decay of $(17.78 \pm 0.10(\text{stat.}) \pm 0.09(\text{syst.})\%$. The branching ratio was calculated using

$$B_e = \frac{N_e^{\text{corr}}}{N_{\tau}(1 - f_{\text{bkgd}}^{\text{non-}\tau})} \frac{1 - f_{\text{bkgd}}^{\text{non-e}}}{\epsilon_E} \frac{1}{F_{\text{bias}}^e}$$

where N_{τ} is the number of taus (165 616), $f_{\text{bkgd}}^{\text{non-}\tau}$ is the background in the tau sample (0.0170 ± 0.0012) and F_{bias}^e is a correction for the slight bias on the branching ratio introduced by the tau pair selection

Table 3
Systematic errors

electron background	0.00058
electron identification selection efficiency	0.00048
bias factor	0.00039
fiducial selection efficiency	0.00028
non-tau background	0.00022
photon conversions	0.00006
Total	0.00093

(1.0036 ± 0.0022). The number of electrons, N_e^{corr} , in the above equation is corrected for the fiducial selection efficiencies (given in Table 2) by

$$N_e^{\text{corr}} = \sum_{i=1}^{10} \frac{N_e^{1ik}(i)}{\epsilon_F^{1ik}(i)} + \frac{N_e^{2ik}}{\epsilon_F^{2ik}} + \frac{N_e^{3ik}}{\epsilon_F^{3ik}}$$

where N_e is the number of electron candidates and ϵ_F is the fiducial selection efficiency. The superscripts indicate the number of charged tracks in the jet. The summation is performed over 10 momentum bins for jets with 1 charged track. The average fiducial selection efficiency for jets with 1 charged track is 0.8395 ± 0.0020 where the error is dominated by the systematic error in the z -chamber hit efficiency. Using the average efficiencies will give a branching ratio similar to the quoted value.

5. Systematic uncertainties

The contributions to the systematic error are given in Table 3. The uncertainty in the efficiency of the electron selection and the uncertainty in the background in the electron sample are discussed in the following paragraphs. The photon conversion systematic error arises as the Monte Carlo has a slightly different probability for a photon conversion from that observed in the data. However since jets with up to three charged tracks are permitted into the sample, the dependence of the final result on this probability was found to be fairly weak.

The electron identification efficiency was determined using Monte Carlo. To test the validity of the Monte Carlo, the efficiency of each criterion in the selection was determined using highly pure control samples of electrons obtained by applying tight cuts to the tau sample. Comparisons of the efficiencies

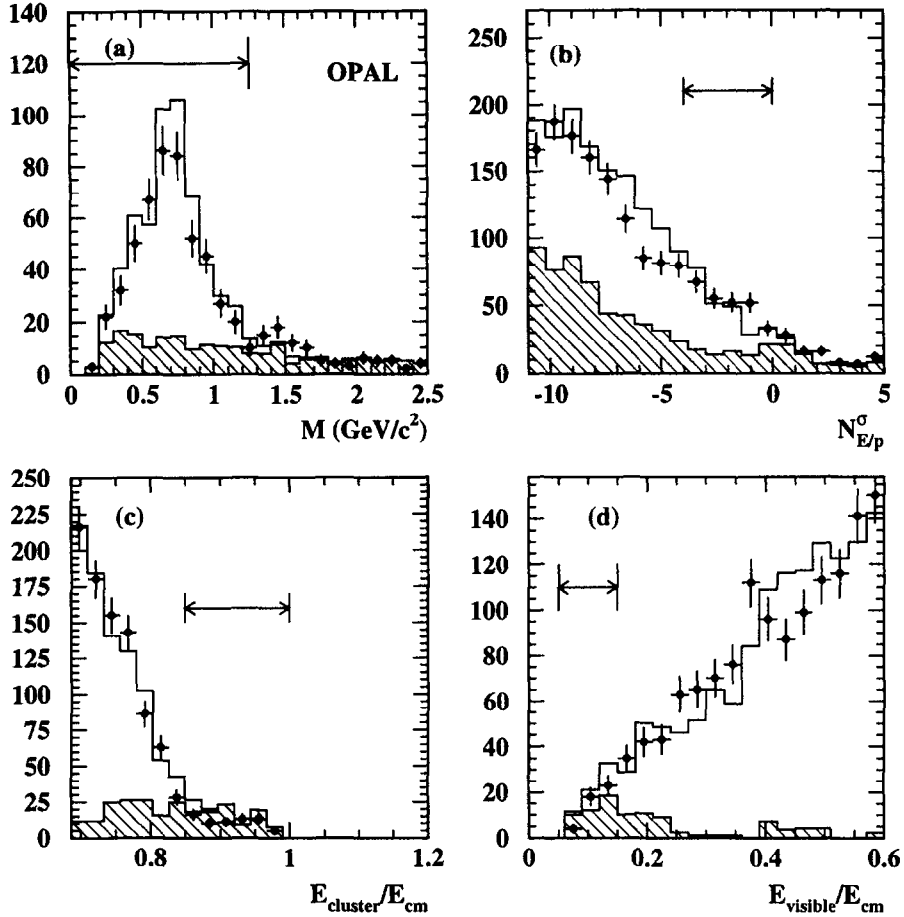


Fig. 2. The distributions used to obtain the background correction factors are shown. The data are represented by the points and the Monte Carlo prediction is represented by the histogram. Figure (a) is the mass distribution used to estimate the $\tau^- \rightarrow h^- \geq 1\pi^0\nu_\tau$ background correction. The unshaded portion of the histogram shows the $\tau^- \rightarrow h^- \geq 1\pi^0\nu_\tau$ decays and shaded portion shows the other tau decays. Figure (b) is the $N_{E/p}^\sigma$ distribution used to estimate the $\tau^- \rightarrow h^- \nu_\tau$ background correction. The unshaded portion shows the $\tau^- \rightarrow h^- \nu_\tau$ decays and shaded portion shows the other tau decays. Figure (c) is the $E_{\text{cluster}}/E_{\text{CM}}$ distribution used to estimate the $e^+e^- \rightarrow e^+e^-$ background correction. The unshaded portion shows the tau decays and the shaded portion shows the $e^+e^- \rightarrow e^+e^-$ events that pass the electron selection. Figure (d) is the $E_{\text{visible}}/E_{\text{CM}}$ distribution used to estimate the $e^+e^- \rightarrow (e^+e^-)e^+e^-$ background correction. The unshaded portion shows the tau decays and the shaded portion shows the $e^+e^- \rightarrow (e^+e^-)e^+e^-$ events where both jets pass the electron selection. The arrows indicate the regions used to determine the correction factors.

obtained from the Monte Carlo and data control samples showed no inconsistencies. For example, we found the efficiency of the dE/dx criterion to be 0.99562 ± 0.00126 and 0.99662 ± 0.00102 in the data and Monte Carlo, respectively. Since the efficiencies from the data and Monte Carlo were in good agreement, we assign a systematic error to the electron identification efficiency of 0.0016 for the dE/dx requirement which is obtained by adding in quadrature the statistical errors of the data and Monte Carlo effi-

ciencies. This procedure was repeated for each criterion and the total uncertainty on the electron identification selection efficiency is estimated to be 0.00048 (see Table 3). Additional checks were made using samples of $e^+e^- \rightarrow e^+e^-$ and $e^+e^- \rightarrow (e^+e^-)e^+e^-$ data. Further, the reliability of the branching ratio was investigated by varying the individual selection requirements. No discrepancies were observed, so no additional uncertainty was added to the efficiency.

The background in the $\tau^- \rightarrow e^- \bar{\nu}_e \nu_\tau$ sample is

described below and presented in Table 1. The backgrounds were first estimated using Monte Carlo samples. The modelling of each of the backgrounds by the Monte Carlo was checked by creating subsamples from the electron candidates enriched in the background.

- (a) $\tau^- \rightarrow h^- \geq 1\pi^0\nu_\tau$ (h^- is either a π^- or K^-). The modelling of this background is studied by examining the jet mass distribution of those events that have one photon candidate (see Fig. 2(a)). The jet mass is calculated using the track information for one four-vector and the cluster direction and energy for the second four-vector (we assume that both particles are pions). A dE/dx requirement is also added which reduces the electrons but not the hadrons from this sample. Comparisons of data and Monte Carlo suggest that the Monte Carlo overestimates the background and we apply a correction of 0.83 ± 0.06 to this background estimate.
- (b) $\tau^- \rightarrow h^-\nu_\tau$. The $\tau^- \rightarrow h^-\nu_\tau$ background was checked by comparing the $N_{E/p}^\sigma$ distribution for data and Monte Carlo (see Fig. 2(b)) for events that passed the electron selection but with the dE/dx requirement reversed so that hadrons instead of electrons were selected. We use the region $-4 \leq N_{E/p}^\sigma \leq 0$, which corresponds to the region included in our selection, to obtain a correction factor of 1.25 ± 0.14 . Although the modelling of the $N_{E/p}^\sigma$ distribution in Fig. 2(b) is not ideal, changing the region used to determine the correction does not change the branching ratio.
- (c) $e^+e^- \rightarrow e^+e^-$. The $e^+e^- \rightarrow e^+e^-$ events that pass the electron selection tend to be events with final state radiation. Unfortunately we found that these $e^+e^- \rightarrow e^+e^-$ events were not well modelled by the Monte Carlo. In Fig. 2(c) we plot $E_{\text{cluster}}/E_{\text{CM}}$ for jets that pass the electron selection. The $e^+e^- \rightarrow e^+e^-$ Monte Carlo overestimates the background and we apply a correction factor of 0.55 ± 0.09 to the background estimate obtained from the Monte Carlo.
- (d) $e^+e^- \rightarrow (e^+e^-)e^+e^-$. A sample of $e^+e^- \rightarrow (e^+e^-)e^+e^-$ events was created by requiring both jets in an event to pass our electron selection. In Fig. 2(d) we plot the ratio $E_{\text{visible}}/E_{\text{CM}}$ where $E_{\text{visible}} = E_{\text{cluster}} + E_{\text{track}}$. We find that the Monte Carlo overestimates the background and we apply a correction factor of 0.7 ± 0.2 .

6. Discussion and summary

The $\tau^- \rightarrow e^-\bar{\nu}_e\nu_\tau$ branching ratio was previously measured by OPAL to be $(18.04 \pm 0.33)\%$ [8] using data collected between 1990 and 1992. The current result, $(17.78 \pm 0.10 \pm 0.09)\%$, is consistent with the previous work, using a quite different selection procedure and with approximately three times the data sample. In addition, the branching ratio is consistent with other results, including recent measurements by ALEPH [13] of $(17.79 \pm 0.12 \pm 0.06)\%$ and DELPHI [14] of $(17.51 \pm 0.39)\%$. The 1994 Particle Data Group average value is $(17.90 \pm 0.17)\%$ [15].

The $\tau^- \rightarrow e^-\bar{\nu}_e\nu_\tau$ branching ratio can be used to test lepton universality. The ratio of the widths for $\tau^- \rightarrow \mu^-\bar{\nu}_\mu\nu_\tau$ and $\tau^- \rightarrow e^-\bar{\nu}_e\nu_\tau$ gives a measure of g_μ/g_e [16]

$$\frac{\Gamma(\tau^- \rightarrow \mu^-\bar{\nu}_\mu\nu_\tau)}{\Gamma(\tau^- \rightarrow e^-\bar{\nu}_e\nu_\tau)} = \frac{g_\mu^2}{g_e^2} \frac{f(m_\mu^2/M_\tau^2)}{f(m_e^2/M_\tau^2)}$$

where g_μ and g_e are the electroweak coupling constants for the muon and electron, and $f(x) = 1 - 8x + 8x^3 - x^4 - 12x^2 \ln x$. Using the latest measurement of the τ mass by the BES Collaboration of $1776.96^{+0.18+0.25}_{-0.21-0.17}$ MeV/ c^2 [17] and the OPAL $\tau^- \rightarrow \mu^-\bar{\nu}_\mu\nu_\tau$ branching ratio of $(17.36 \pm 0.27)\%$ [8], we obtain $g_\mu/g_e = 1.0016 \pm 0.0087$. Note, however, that the most precise test of this universality (at the level of 0.002) has been made by measuring the pion leptonic branching ratios [18].

A test of muon-tau universality can be made by comparing the partial widths for the $\tau^- \rightarrow e^-\bar{\nu}_e\nu_\tau$ and $\mu^- \rightarrow e^-\bar{\nu}_e\nu_\mu$ decays, which have the form [16]

$$\frac{g_\tau^2}{g_\mu^2} = 0.9996 \frac{\tau_\mu}{\tau_\tau} \frac{m_\mu^5}{m_\tau^5} B(\tau^- \rightarrow e^-\bar{\nu}_e\nu_\tau)$$

Using the OPAL tau lifetime measurement of $288.8 \pm 2.2 \pm 1.4$ fs [19], we obtain $g_\tau/g_\mu = 1.0025 \pm 0.0060$. The OPAL tau lifetime and $\tau^- \rightarrow e^-\bar{\nu}_e\nu_\tau$ branching ratio are plotted in Fig. 3. The band is the Standard Model prediction assuming lepton universality. The width of the band corresponds to the uncertainty in the tau mass.

The strong coupling α_s can be extracted from $R_\tau = B(\tau^- \rightarrow \text{hadrons}^-\nu_\tau)/B(\tau^- \rightarrow e^-\bar{\nu}_e\nu_\tau)$ using the leptonic branching ratios and the τ lifetime. In an earlier OPAL publication, $R_\tau = 3.654 \pm 0.038$ was determined using the leptonic branching ratio

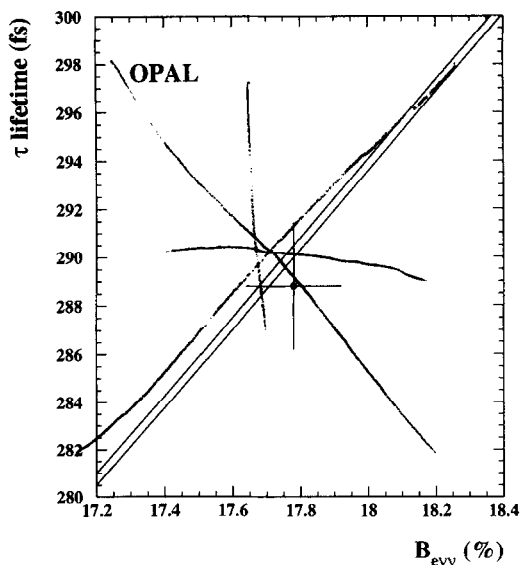


Fig. 3. The electronic branching ratio of the tau is plotted against the OPAL tau lifetime. The band is the prediction assuming $\mu - \tau$ universality and its width reflects the uncertainty associated with the tau mass.

based on 1990–1992 data [8] and the lifetime based on 1990–1993 data [19]. We follow the same prescription that was described in detail in Ref. [8]. Our new measurement of $B(\tau^- \rightarrow e^- \bar{\nu}_e \nu_\tau)$, together with the τ lifetime and $\tau^- \rightarrow \mu^- \bar{\nu}_\mu \nu_\tau$ branching ratio, gives $R_\tau = 3.659 \pm 0.030$. The resulting α_s value is $0.377^{+0.015+0.026}_{-0.014-0.018}$ at $Q^2 = M_\tau^2$ and $0.1231 \pm 0.0013^{+0.0025}_{-0.0021}$ at $Q^2 = M_Z^2$ where the first error is experimental and the second error is theoretical. Note, however, there may be an additional uncertainty of as much as ± 0.002 [20] or ± 0.005 [21] from effects beyond the SVZ parameterization [22] used to determine the coupling constant.

In summary, the branching ratio of the $\tau^- \rightarrow e^- \bar{\nu}_e \nu_\tau$ decay was measured using the 1991–1994 data samples recorded using the OPAL detector to be

$$B(\tau^- \rightarrow e^- \bar{\nu}_e \nu_\tau) = (17.78 \pm 0.10 \pm 0.09)\%$$

This new branching ratio supersedes the previous OPAL measurement and is consistent with the results of other experiments. The branching ratio has been used together with other measurements to test $e - \mu$ and $\mu - \tau$ lepton universality. The results indicate that the hypotheses of lepton universality in the charged current weak interaction are valid to within the 1% level.

Acknowledgements

It is a pleasure to thank the SL Division for the efficient operation of the LEP accelerator, the precise information on the absolute energy, and their continuing close cooperation with our experimental group. In addition to the support staff at our own institutions we are pleased to acknowledge the Department of Energy, USA, National Science Foundation, USA, Particle Physics and Astronomy Research Council, UK, Natural Sciences and Engineering Research Council, Canada, Fussesfeld Foundation, Israel Ministry of Science, Israel Science Foundation, administered by the Israel Academy of Science and Humanities, Minerva Gesellschaft, Japanese Ministry of Education, Science and Culture (the Monbusho) and a grant under the Monbusho International Science Research Program, German Israeli Bi-national Science Foundation (GIF), Direction des Sciences de la Matière du Commissariat à l’Energie Atomique, France, Bundesministerium für Forschung und Technologie, Germany, National Research Council of Canada, A.P. Sloan Foundation and Junta Nacional de Investigação Científica e Tecnológica, Portugal, Hungarian Foundation for Scientific Research, OTKA T-016660.

References

- [1] OPAL Collaboration, K. Ahmet et al., Nucl. Instr. Meth. A 305 (1991) 275.
- [2] S. Jadach, B.F.L. Ward, and Z. Was, Comp. Phys. Comm. 79 (1994) 503; (KORALZ Version 4.0).
- [3] S. Jadach, J.H. Kühn, and Z. Was, Comp. Phys. Comm. 76 (1993) 361; (TAUOLA Version 2.0).
- [4] R. Brun et al., GEANT 3, Report DD/EE/84-1, CERN (1989).
- [5] J. Allison et al., Comp. Phys. Comm. 47 (1987) 55.
- [6] OPAL Collaboration, G. Alexander et al., Phys. Lett. B 266 (1991) 201.
- [7] OPAL Collaboration, P. Acton et al., Phys. Lett. B 288 (1992) 373.

- [8] OPAL Collaboration, R. Akers et al., *Z. Phys. C* 66 (1995) 543.
- [9] OPAL Collaboration, G. Alexander et al., *Z. Phys. C* 52 (1991) 175.
- [10] M. Böhm, A. Denner and W. Hollik, *Nucl. Phys. B* 304 (1988) 687;
F.A. Berends, R. Kleiss, W. Hollik, *Nucl. Phys. B* 304 (1988) 712; (BABAMC).
- [11] T. Sjöstrand, *Comp. Phys. Comm.* 39 (1986) 347;
T. Sjöstrand, *Comp. Phys. Comm.* 43 (1987) 367;
T. Sjöstrand, CERN-TH-6488/92; (JETSET, Version 7.3).
- [12] R. Bhattacharya, J. Smith, G. Grammer, *Phys. Rev. D* 15 (1977) 3267;
J. Smith, J.A.M. Vermaseren, G. Grammer, *Phys. Rev. D* 15 (1977) 3280; (Vermaseren, Version 1.01).
- [13] ALEPH Collaboration, D. Buskulic et al., CERN Preprint CERN-PPE/95-127.
- [14] DELPHI Collaboration, P. Abreu et al., CERN Preprint CERN-PPE/95-114.
- [15] Review of Particle Properties, L. Montanet et al., *Phys. Rev. D* 50 (1994) 1173.
- [16] W.J. Marciano and A. Sirlin, *Phys. Rev. Lett.* 61 (1988) 1815.
- [17] BES Collaboration, J.Z. Bai et al., SLAC Preprint SLAC-PUB-6930.
- [18] D. Britton et al., *Phys. Rev. Lett.* 68 (1992) 3000.
G. Czapek et al., *Phys. Rev. Lett.* 70 (1993) 17.
- [19] OPAL Collaboration, R. Akers et al., *Phys. Lett. B* 338 (1994) 497.
- [20] S. Narison, Proc. Third Workshop on Tau Lepton Physics, Montreux (1994), CERN-TH 7506 (1994)
- [21] G. Altarelli, P. Nason and G. Ridolphi, CERN-TH 7537 (1994)
- [22] M.A. Shifman, A.L. Vainstein and V.I. Zakharov, *Nucl. Phys. B* 147 (1979) 385, 448, 519.